Environmental Research 244 (2024) 117902

Contents lists available at ScienceDirect

Environmental Research

journal homepage: www.elsevier.com/locate/envres

Using live videography observation and Bayesian isotope mixing model to identify food composition and dietary contribution to inorganic mercury and methylmercury intake by songbird nestlings

Shenghao Li [a], Fudong Zhang [b], Zhidong Xu [c], Dongya Jia [a], Gaoen Wu [d], Hongjiang Liu [a], Chan Li [e], Longchao Liang [a], Jiemin Liu [f], Zhuo Chen [a,**], Guangle Qiu [c,*]

[a] School of Chemistry and Materials Science, Guizhou Normal University, Guiyang, 550001, China
[b] College of Resources and Environmental Engineering, Guizhou University, Guiyang, 550025, China
[c] State Key Laboratory of Environmental Geochemistry, Institute of Geochemistry, Chinese Academy of Sciences, Guiyang, 550081, China
[d] State Key Laboratory of Marine Resource Utilization in South China Sea, Hainan University, Haikou, 570228, China
[e] School of Ecology and Environmental Science, Yunnan University, Kunming, 650091, China
[f] Guizhou Provincial People's Hospital, Guiyang, 550002, China

ARTICLE INFO

Keywords:
Food compositions
Dietary intakes of inorganic mercury and methylmercury
Green-backed tit nestlings
Live videography observation
Bayesian isotopic mixing model

ABSTRACT

Mercury (Hg) exposure is increasing in terrestrial birds; however, studies on its sources are scarce. In the present study, we elucidated the food composition of green-backed tit nestlings from three urban forest parks (CPL, AHL, and LCG) using live videography observation (LVO). Furthermore, the daily dietary intakes of inorganic Hg (IHg) (MDI_{IHg}) and methylmercury (MeHg) (MDI_{MeHg}) were determined using the Bayesian isotope mixing model (BIMM) to uncover the nestlings' specific dietary Hg contribution. Both LVO and BIMM indicated that Lepidoptera (primarily caterpillar) constituted the primary food source for the nestlings in the three forests, accounting for approximately 60% of their diet in all three forest parks. The estimated MDI of Hg revealed that lepidopterans and spiders primarily contributed to IHg exposure, with a co-contribution ratio of 71.8%–97.7%. Unexpectedly, dietary MeHg was mostly derived from spiders; the highest contribution ratio of 93.6% was recorded at CPL, followed by another peak ratio of 92.9% at LCG. However, the dietary exposure was primarily IHg, accounting for 69.8% (AHL), 62.0% (LCG), and 61.3% (CPL) of the nestlings. Our study findings highlight the importance of dietary IHg transfer in evaluating the effects of Hg in nestlings. LVO, coupled with BIMM, is an effective tool for determining the food compositions of songbird nestlings and estimating the contribution of specific diets.

1. Introduction

Mercury (Hg) is a persistent toxic metal that can be transported as gaseous forms (primarily Hg^0) over a long distance in the atmosphere, resulting in widespread environmental distribution (Driscoll et al., 2013). Due to significant atmospheric diffusion and its high toxicity, Hg has been defined as a global pollutant by the World Health Organization and included in the list of the top 10 chemicals of public health concern (Lindqvist et al., 1991; WHO, 2020). Atmospheric Hg eventually enters the surface environment via wet and dry deposition. Once the inorganic Hg (IHg) of gaseous Hg^0 and Hg^{2+} are deposited into the environment, they can be readily converted to the highly neurotoxic organic form, i.e., methylmercury (MeHg), by microbes under certain conditions. MeHg has a high degree of bioavailability and bioaccumulation; therefore, it can be significantly biomagnified in organisms via the food chain (Cristol et al., 2008; Tsui et al., 2012). Several studies have reported that extremely high MeHg levels can accumulate in the top consumers of aquatic food chains, highlighting the significant accumulation and biomagnification of MeHg in the aquatic biota (Hall et al., 2020; Lavoie et al., 2013; Ponton et al., 2021; Zabala et al., 2019).

While the majority of studies on Hg transfer in food chains have traditionally concentrated on aquatic ecosystems, there has been a growing body of research over the past two decades that has shown the bioaccumulation and biomagnification of Hg in terrestrial food chains.

* Corresponding author.
** Corresponding author.
E-mail addresses: chenzhuo19@163.com (Z. Chen), qiuguangle@mail.gyig.ac.cn (G. Qiu).

https://doi.org/10.1016/j.envres.2023.117902
Received 16 October 2023; Received in revised form 30 November 2023; Accepted 7 December 2023
Available online 12 December 2023

For example, Abeysinghe et al. (2017) reported an extremely high Hg concentration of 123.3 ± 34.2 mg/kg in the feathers of spot-breasted scimitar babbler (*Pomatorhinus mcclellandi*) inhabiting a Hg-contaminated area; this value was considerably higher than the highest Hg concentration of 91.6 mg/kg measured in the feathers of the wandering albatross (*Diomedea exulans*) (Renedo et al., 2017). Recently, a risk level of 5.3 mg/kg Hg (>1.8 times the threshold for detrimental health effects on songbirds, Jackson et al., 2011a) was observed in the feathers of grey-headed canary-flycatcher (*Culicicapa ceylonensis*) living in a remote forest ecosystem (Li et al., 2021). Compared with the aquatic food diets of waterbirds, the food diets of terrestrial birds are more complex, with varying Hg exposure pathways. Therefore, identifying the food sources and determining diet-specific Hg contribution are particularly vital for understanding the high Hg concentrations in terrestrial birds.

Green-backed Tit (*Parus monticolus*) as a model species is frequently employed for studying Hg exposure due to their limited habitat range, widespread distribution, insect-eating habits, and the ease of monitoring them in artificial nest boxes during the breeding season (Xu et al., 2023a). Throughout the breeding season, the parent Green-backed Tit primarily feed their nestlings with Lepidoptera larvae (caterpillars), spiders, and other invertebrates from various trophic levels (García--Navas et al., 2015; Tomasz and Grzegorz, 2017; Sinkovics et al., 2021). Since feathers Hg as a reliable indicator of birds' Hg exposure, the accumulation of Hg in nestling feathers can provide insights into Hg exposure during their growth stage.

Using an artificial nest box coupled with live videography observation (LVO) is an efficient method for investigating the breeding behavior and environmental pollutant exposure of cavity-nesting birds (Surmacki and Podkowa, 2022). High-resolution cameras installed inside nest boxes can directly and continuously observe and record incubation data, including the food types and feeding frequencies of nestlings (Iezekiel et al., 2021); as a result, the proportions of the food sources of nestlings can be estimated. For example, Pagani-Núñez et al. (2017) successfully used infrared motion cameras to estimate the dietary compositions of great tit nestlings. Furthermore, Hartman et al. (2019) monitored the incubation behavior of tree swallows and observed that females with higher Hg concentrations decreased their brood-rearing period, resulting in adverse effects on reproduction. Furthermore, Sinkovics et al. (2021) conducted a comparison of the food compositions of great tit nestlings in both urban and forest habitats, utilizing video records. Recently, Luo et al. (2020) and Zhang et al. (2022) used nest boxes, established the food chains of pine forest birds, and revealed Hg accumulation and biomagnification. Therefore, LVO can serve as a feasible tool to solve the challenges of complex food composition and diverse exposure routes in studies on the food chains of terrestrial birds.

Stable isotopes of carbon ($\delta^{13}C$) and nitrogen ($\delta^{15}N$) are widely used to identify food sources and the trophic position of biota in food chains (Hyodo, 2015; Post, 2002). $\delta^{13}C$ is generally used to distinguish different sources/origin of carbon since different sources/origin (e.g., terrestrial vs aquatic, C3 vs C4, etc.) that have different carbon isotope compositions. Because of the insignificant fractionations of $\delta^{13}C$ ($\Delta^{13}C \approx 0.4‰ \pm 1.3‰$) between pray and predators, namely, little changes in food chains, $\delta^{13}C$ can be also elucidated the energy flow to consumers in both terrestrial and aquatic ecosystems. When the isotopic characteristics of carbon sources are different, the carbon source of organisms can be assessed in food chains. Unlikely, the $\delta^{15}N$ value generally increases with trophic levels; furthermore, its fractionation value ($\Delta^{15}N$) between consumers and their food is significant ($\sim 3.4‰ \pm 1‰$). Therefore, it is frequently used to evaluate the trophic position of organisms (Post, 2002). Moreover, based on the $\delta^{13}C$ and $\delta^{15}N$ compositional features of consumers and their identified food sources, the contribution portions of different food sources to consumers can be evaluated using the Bayesian isotope mixture model (BIMM) (Parnell et al., 2010, 2013). This method has been successfully used to elucidate the diet composition of birds, including raptors (Robinson et al., 2018) and songbirds (Ai et al., 2019; Pagani-Núñez et al., 2017; White and Dawson, 2021; Xu et al., 2023a).

In the present study, we used an artificial nest box and LVO in urban pine forests to induce bird breeding and identifying the food diets of nestlings. BIMM was employed to ascertain the contribution portions of the identified food diets and the diet-specific Hg loads to nestlings. The objectives were as follows: (1) identify the food compositions and proportions of nestlings; (2) elucidate Hg accumulation and exposure risk in urban forest birds; and (3) estimate the daily dietary intakes of IHg and MeHg (MDI_{IHg} and MDI_{MeHg}, respectively) and diet-specific Hg loads to nestlings.

2. Materials and methods

2.1. Study area

The parks selected for field investigation were as follows: Changpoling National Forest Park (CPL, 106°68′E, 26°67′N), Aha Lake National Wetland Park (AHL, 106°65′E, 26°53′N), and Luchongguan Forest Park (LCG, 106°70′E, 26°63′N). These parks are present in Guiyang, Guizhou Province, Southwest China (Fig. 1). The dominant vegetation types in the three parks are *Pinus armandii* Franch, *Pinus hunbergia* Parl, and *Pinus massoniana* Lamb.

Approximately 300 artificial nest boxes were placed in the pine forests in all three parks. The process of installing nest boxes is summarized in Supplementary Information (**SI**). No apparent water sources were evident in the vicinity of the nest box placement sites at CPL. Nonetheless, a small reservoir is located near AHL and LCG. Therefore, in these two parks, the nest box placement sites were selected sufficiently far away (>200 m) from aquatic habitats to minimize the effects of the aquatic origin of MeHg (Tsui et al., 2014).

2.2. Sample collection and preparation

2.2.1. Live videography observation (LVO)

During the Green-backed Tit (*Parus monticolus*) breeding period, nest boxes were inspected every week. Once the birds laid eggs in the nest box, the investigation period was adjusted to every 3 days. The species of occupied birds, number of eggs laid, and number of hatchlings were recorded.

A portable HD 4K motion camera (Mi Technology, China) was installed inside the selected bird breeding nest box for videographic observations of the feeding behavior of parental nestlings (Fig. S1). Video recordings were performed during 8 a.m.–12 p.m. and 2 p.m.–5 pm; The hot midday period was avoided, when feeding was low. The duration of a single video recording was 2 h; this period can be sufficient to describe the feeding behavior of nestlings (Pagani-Núñez and Senar, 2013). Long recordings were avoided to decrease interference with parental feeding.

A nest box situated in an open area was selected for video recording to ensure video clarity and precise food identification. The nest box selected for recording typically had nestlings aged >5 days to prevent the occurrence of parental abandonment caused by human interference. A total of 28 nest boxes were recorded for a cumulative duration of 117 h over three years, and each of them recorded 2–4 times. Videographic recordings were made in all 3 years, but most concentrated in 2020. All video recordings were dated and numbered for further food species identification. More information about the LVO method were presented in **SI**.

2.2.2. Sampling and preparation

Nestling feathers and invertebrates were collected during the bird breeding season from April to July 2020, 2021, and 2022. In total, 301 individual (64 broods) feather samples of green-backed tit nestlings were collected from the three forest parks, with 185 (38 broods) from CPL, 31 (7 broods) from AHL, and 85 (19 broods) from LCG. We sampled the feathers of all nestlings individually in each clutch. In brief, nestlings

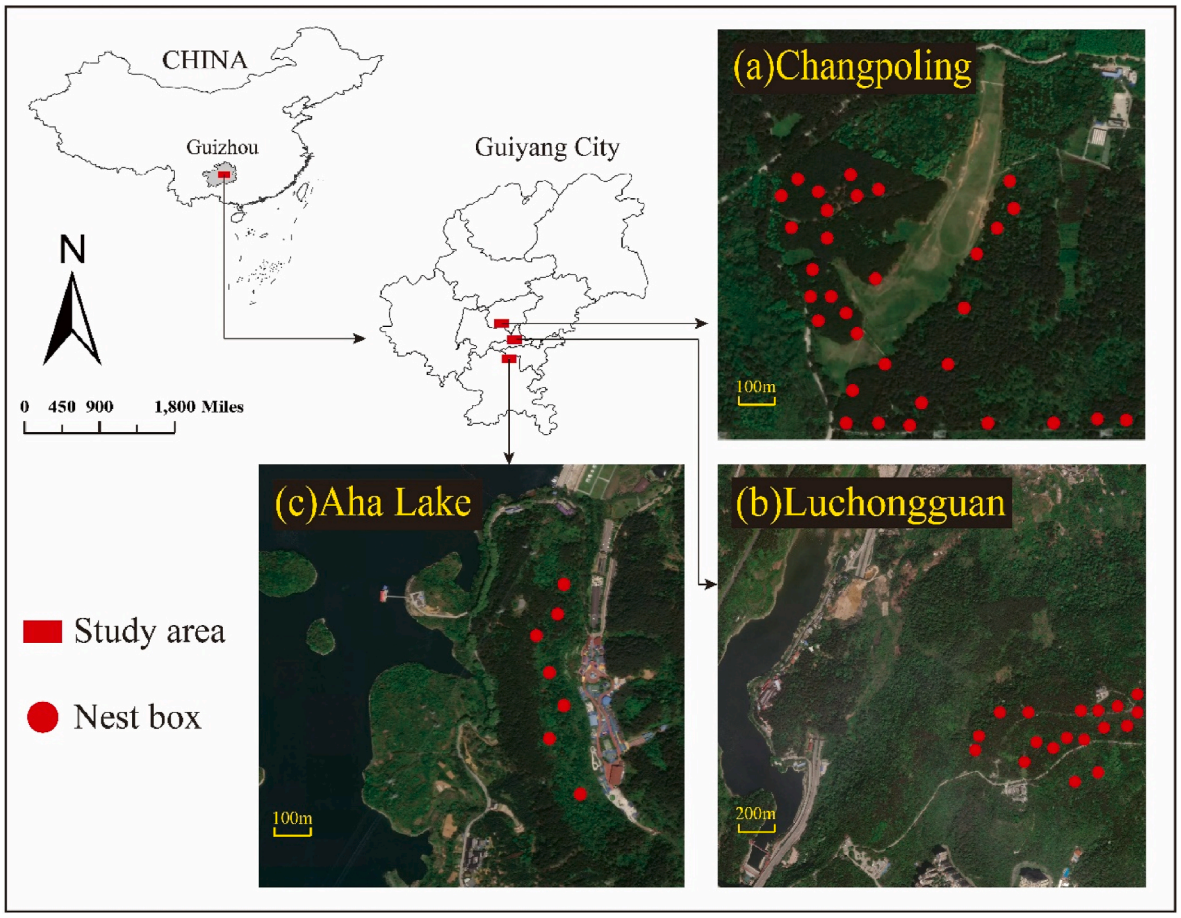

Fig. 1. Sampling sites in Guiyang city urban forest. Red rectangles were study areas, and red dots indicated occupied nest boxes. (a) Changpoling Forest Park; (b) Luchongguan Forest Park; (c) Aha Lake National Wetland Park.

of approximately 14 days old were gently moved from the nest box to a ventilated cloth bag and their weight was measured. Subsequently, the secondary flight feathers on both sides were collected in a clean polyvinyl chloride ziplock bag. After the collection, the nestlings were allowed to rest for a short period and then safely returned to the nest box. Follow-up inspections revealed that all sampled nestlings successfully left the nest, indicating that the noninvasive sampling method did not affect the subsequent normal activities of the nestlings. Feather samples were transported to the laboratory and thoroughly cleaned with detergent and deionized water in an ultrasonic cleaner, air-dried in a cool ventilated place, and bagged for the subsequent processes (Luo et al., 2020; Zhang et al., 2022).

The invertebrates observed by LVO were gathered from the adjacent habitats of the sampled birds during the breeding season using the sweeping web method. During each sampling campaign, we selected at least 3 sub-sites within each site to collect invertebrates, ensuring the randomness of invertebrates. The numbers within the following brackets indicate the total number of final samples (each final sample was composed of at least 10 individual subsamples) from all three sites. The invertebrates included caterpillars (*Lepidoptera*, n = 14), moths (*Moth*, n = 11), spiders (*Araneae*, n = 33), grasshoppers (*Acrida cinerea*, n = 30), katydids (*Longhorned grasshoppers*, n = 16), and mantis (*Mantodea*, n = 17). The individuals were collected and stored in 50 mL centrifuge tubes with sealed gauze, placed in a cooler with ice packs, and transported to the laboratory. All sampled invertebrates were left for 24 h to eliminate their excrements and remnants of food in the digestive system, as these could potentially influence the chemical analyses. Afterward, samples were meticulously rinsed with deionized water, humanely sacrificed, and subjected to freeze-drying. Thereafter, the samples were ground to powder using an agate mortar and pestle and stored in ziplock bags for analysis (Luo et al., 2020; Zhang et al., 2022). All sampled species are not listed in the National List of Key Wildlife.

2.3. Analytical methods

2.3.1. Analysis of total Hg (THg) and MeHg

Owing to the low mass of the feathers and invertebrates, an acid digestion method for simultaneously measuring THg and MeHg was modified based on the methods described by Hammerschmidt and Fitzgerald (2005), Hintelmann and Nguyen (2005), and Tsui et al. (2018, 2019), which have been validated in our previous studies (Xu et al., 2023a; Zhang et al., 2022). In summary, about 0.005–0.010 g of feathers and 0.05–0.10 g of invertebrates was measured and placed into a 50 mL centrifuge tube. Subsequently, 5 mL of 4.6 M HNO3 was added, and the tube was subjected to digestion in a 60 °C oven for 24 h. The tube was shaken every 2 h during this period to ensure thorough digestion, and it remained completely sealed throughout the process.

For MeHg analysis, 2 mL of the above digestion solution was pipetted into a 15 mL centrifuge tube and placed in a water bath at 60 °C for 30 min. Thereafter, an appropriate amount of the water-bathed digestion solution was taken and added to a bubble vial, followed by the addition of sodium acetate buffer solution (2 M, 0.2 mL) to adjust the pH and ethylation with $NaBEt_4$. Then, an appropriate amount of the solution was taken, and MeHg content was measured via gas chromatography–cold vapor atomic fluorescence spectrometry (GC–CVAFS, Brooks Rand Model III, USA) according to the USEPA Method 1630 (US EPA, 1998).

For THg analysis, the remaining part of the digestion solution was

added to 3 mL of concentrated HNO_3 for further digestion in a water bath at 95 °C for 3 h. Then, 0.5 mL of BrCl was added to the solution, and the volume was fixed to 25 mL. The solution was allowed to fully oxidize for 24 h. Then, $NH_2OH{\cdot}HCl$ was added for neutralization, followed by $SnCl_2$ reduction. Lastly, an appropriate aliquot was pipetted into a bubbler for measuring THg levels via CVAFS (Brooks Rand Model III, USA) according to the USEPA Method 1631 (US EPA, 2002).

2.3.2. Quality assurance and quality control (QA/QC)

Method blanks, duplicate samples, and certified materials were used to conduct QA/QC of the analytical data for THg and MeHg. TORT-2 (lobster hepatopancreas, THg certified value: 270 ± 60 ng/g; MeHg certified value: 152 ± 13 ng/g) and human hair (GBW07601a, THg certified value: 670 ± 100 ng/g) were used as the biological samples. The THg recoveries for TORT-2 and human hair were 95.2% ± 5.1% (range: 92.1%–103.2%, n = 15) and 102.9% ± 4.9% (range: 95.3%–109.9%, n = 9), respectively. The MeHg recovery for TORT-2 was 96.7% ± 5.1% (range: 87.3%–101.6%, n = 6). In addition, the RSDs were 5.3% (THg) and 5.3% (MeHg) for TORT-2 and 4.7% (THg) for human hair (Table S1).

2.3.3. Stable isotope analysis

The stable $\delta^{13}C$ and $\delta^{15}N$ compositions of the nestling feathers and invertebrates were measured at the State Key Laboratory of Environmental Geochemistry, Institute of Geochemistry, Chinese Academy of Sciences. An elemental analyzer (EA-2000, Thermo Fisher Inc., USA) along with a gas isotope mass spectrometer (MAT-253, Thermo Fisher Inc.) as well as the rapid combustion method were used to determine the $\delta^{13}C$ and $\delta^{15}N$ compositions in the samples. Around 100 μg of the samples for δ13C and 400 μg for δ15N were carefully measured into a tin cup for isotopic composition analysis. The test's precision was within <0.1‰, and the outcomes were reported in per mil (‰):

$$\delta R_{sample} = \left(R_{sample}/R_{standard} - 1\right) \times 1000 \quad (1)$$

Where R represents $\delta^{13}C$ or $\delta^{15}N$ and R_{sample} and $R_{standard}$ represent the carbon and nitrogen isotopic abundance ratios ($^{13}C/^{12}C$ and $^{15}N/^{14}N$) in the samples and standards, respectively. The isotopic standards of $\delta^{13}C$ and $\delta^{15}N$ were cellulose IAEA-C3 ($\delta^{13}C = -24.9‰$) and ammonium sulfate IAEA-N1 ($\delta^{15}N = 0.4‰$). They were converted into the international common reference values of V-PDB for carbon and standard atmospheric nitrogen for nitrogen, respectively. In the present study, green-backed tit nestling feathers (n = 36), spiders (n = 9), Lepidoptera (n = 22, with 13 caterpillars and 9 moths), Orthoptera (n = 14, with 8 grasshoppers and 6 katydids), and Mantises (n = 11) were selected for $\delta^{13}C$ and $\delta^{15}N$ ratio analysis.

2.4. Trophic structure of the food webs and identification of nestling food items

2.4.1. Trophic structure

Stable Isotope Bayesian Ellipses in R was used to determine Layman's community metrics (Layman et al., 2007) to assess the trophic structure of the food webs in the three parks based on the $\delta^{13}C$ and $\delta^{15}N$ values of the predators (birds) and preys (invertebrates) in these parks.

Seven ecological metrics were calculated to quantify the trophic structure of the food webs (Hilgendag et al., 2022; Jackson et al., 2011b; Layman et al., 2007): $\delta^{15}N$ range (NR, representing trophic level length), $\delta^{13}C$ range (CR, representing diversity in basal carbon sources), mean distance to centroid (CD, representing average trophic diversity), mean nearest neighbor distance to centroid (MNND, representing trophic ecological redundancy), standard deviation of nearest neighbor distance to centroid (SDNND, representing trophic distribution evenness), total area enclosed by the isotopic values of all species (TA, representing total isotopic niche space), and standard ellipse area-corrected (SEAc, indicating the use of ecological space by organisms).

2.4.2. Identification of nestling food items and calculation of contributing rates

Field video recording data were used to preliminarily identify the food items fed to the nestlings by their parents. Subsequently, the "simmr" function in R was employed to compute the proportion of each identified food item contributing to nestlings. The trophic enrichment factors (TEF) of $\Delta^{13}C$ (1.9‰ ±0.1‰) and $\Delta^{15}N$ (3.2‰ ±0.1‰) between food items and great tit nestling feathers (Pagani-Núñez et al., 2017) were referred to represent the TEF between the items of green-backed tit nestlings and preys. The Markov chain Monte Carlo algorithm was used to determine the contribution ratios of each food source.

2.4.3. Nestling dietary intake and proportional Hg contribution

Estimation of food intake. The daily food intake rate (DIR, g/day, dry weight) of the birds was estimated using the conventional equation of the body weight (W, g, Table S2) of the birds. This method was originally described by Agency (1993) and has been applied to various songbirds in a study conducted by Wu et al. (2022). The daily food intake (DFI, g/day, dry weight) of each food item (Ai et al., 2019) was calculated based on the contribution ratio (ρ_i) of the food item I obtained from BIMM.

The corresponding equations are as follows:

$$DIR = 0.648W^{0.651} \quad (2)$$

$$DFI = DIR \times \rho_i \quad (3)$$

$$\Sigma\rho_i = 1 \quad (4)$$

$$\Sigma DFI = DIR \quad (5)$$

Proportional Hg contribution. The contribution of the food item I to the total dietary Hg of the nestling (Y_i) was calculated as follows:

$$MDI = C \times DFI \quad (6)$$

$$Y = MDI / \Sigma MDI \quad (7)$$

Where MDI represents the daily Hg intake from each food item (ng/day); C represents the Hg concentration in each food item (including THg, MeHg, and IHg); and ΣMDI represents the sum of the masses of all food items of Hg (ng).

2.5. Statistical analysis and graphing

Origin Pro 2023 (Origin Lab Inc., USA) and GraphPad Prism 9 (GraphPad Software., USA) were used to perform data analysis, statistical analysis, and mapping. The raw data underwent assessments for normality of distribution and homogeneity of variance using the D'Agostino-Pearson test and Brown-Forsythe test, respectively. Ordinary one-way ANOVA was employed to examine differences ($p < 0.05$) in feather concentration and carbon/nitrogen isotopes. ArcGIS 10.2 (ESRI Inc., USA) and Adobe Illustrator (Adobe Inc., USA) were used to create the sampling sites and study regions. The R language platform (R Team, 2023) was used to determine food web structure metrics and nestling food composition.

3. Results

3.1. Urban pine forest food webs

3.1.1. Stable isotope compositions

There were variations in the $\delta^{15}N$ values of green-backed tit nestling feathers among the three parks, with the highest average value of 4.03‰ ± 0.50‰ observed at CPL, which was similar to LCG (3.58‰ ± 0.44‰) ($p > 0.05$), but significantly higher at AHL (2.35‰ ± 0.53‰) ($p < 0.0001$) (Table 1 and Fig. 2a). In CPL and LCG, the lowest $\delta^{15}N$ values were found for Orthoptera, measuring 0.91‰ ± 0.94‰ and 0.53‰ ±

Table 1
Carbon and nitrogen isotopic compositions and the concentrations of THg, MeHg and MeHg% in different samples from CPL, LCG and AHL.

Site	Sample	$\delta^{13}C$‰		$\delta^{15}N$‰		THg(ng/g)			MeHg(ng/g)			MeHg%
		Mean ± SD	N	Mean ± SD	N	Mean ± SD	Range	N	Mean ± SD	Range	N	Mean ± SD
CPL	Green-backed Tit	−25.6 ± 0.57	12	4.03 ± 0.50	12	486 ± 151	231–1291	185	158 ± 47	70–405	185	34 ± 8.6
	Lepidoptera	−30.9 ± 0.90	6	0.96 ± 1.58	6	54 ± 27	32–98	6	2.7 ± 1.4	1.4–4.9	6	5.0 ± 0.9
	Spider	−25.5 ± 0.17 [a]	3	5.06 ± 0.69 [a]	3	353 ± 123	100–527	23	191 ± 98	51–351	23	53 ± 17
	Orthoptera	−26.2 ± 1.91	5	0.91 ± 0.94	5	8.4 ± 2.2 [a]	6.4–13.9 [a]	19	0.6 ± 0.3 [a]	0.3–1.0 [a]	19	7.8 ± 3.9 [a]
	Mantis	−20.6 ± 1.67	5	3.29 ± 0.27	5	30 ± 5.6 [a]	23–36 [a]	4	17 ± 5.0 [a]	13–24 [a]	4	56 ± 8.9 [a]
LCG	Green-backed Tit	−25.0 ± 0.32	12	3.58 ± 0.44	12	564 ± 163	216–1006	85	249 ± 109	104–596	85	45 ± 16
	Lepidoptera	−30.5 ± 1.73	8	0.73 ± 0.21	8	69 ± 57	22–173	7	3.0 ± 1.4	1.4–5.4	7	5.6 ± 1.9
	Spider	−26.3 ± 0.88	3	4.14 ± 0.04	3	363 ± 101	263–523	5	211 ± 53	263–523	5	59 ± 12
	Orthoptera	−22.5 ± 1.58	6	0.53 ± 0.34	6	28 ± 11	15–53	13	2.0 ± 1.3	1.0–4.4	6	6.4 ± 1.5
	Mantis	−21.2 ± 0.47	3	2.69 ± 0.18	3	145 ± 82	79–272	5	22 ± 1.8	20–25	5	18 ± 7.9
AHL	Green-backed Tit	−25.0 ± 0.70	12	2.35 ± 0.53	12	491 ± 84	310–669	31	239 ± 71	106–405	31	48 ± 9.6
	Lepidoptera	−30.0 ± 1.26	8	−0.66 ± 1.36	8	63 ± 41	22–125	12	8.5 ± 5.7	1.9–18	12	24 ± 20
	Spider	−25.0 ± 0.54	3	5.53 ± 0.20	3	291 ± 46	261–371	5	141 ± 14	126–157	5	49 ± 5.1
	Orthoptera	−22.4 ± 0.58	3	0.88 ± 0.36	3	25 ± 7.1	10–35	14	1.2 ± 0.4	0.7–1.9	7	4.8 ± 1.6
	Mantis	−26.9 ± 0.58	3	2.22 ± 0.58	3	120 ± 18	96–151	8	48 ± 11	35–62	6	39 ± 4.7

[a] Data from Zhang et al. (2022).

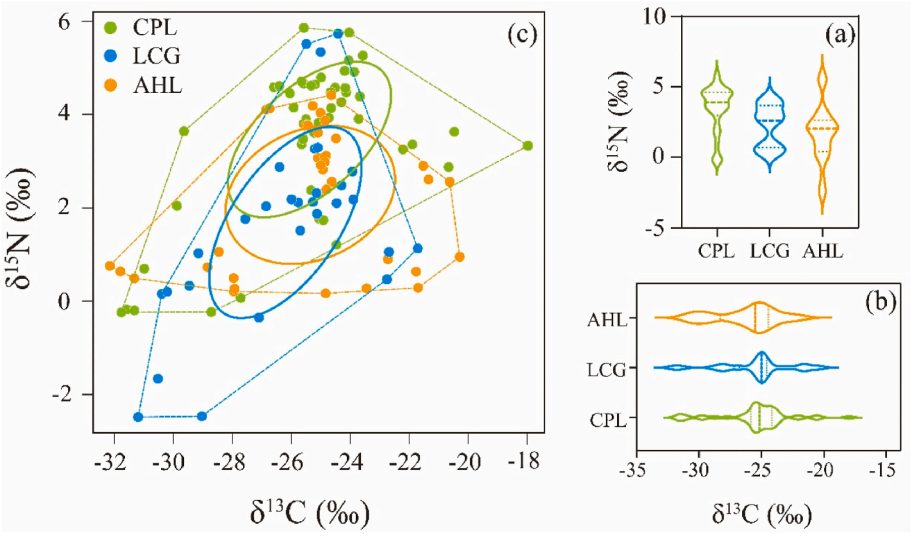

Fig. 2. Carbon and nitrogen isotope compositions from different parks. (a) Stable nitrogen isotope ($\delta^{15}N$) composition: the thicker dashed lines indicated the mean values for $\delta^{15}N$; (b) Stable carbon isotope ($\delta^{13}C$) composition: the thicker dashed lines indicated the mean values for $\delta^{13}C$. (c) Bi-plotted $\delta^{13}C$ and $\delta^{15}N$: the shaded part indicated the corrected Bayesian standard elliptical area (SEAc) and the dashed line indicates the total area (TA) of the area surrounded by isotopic values for all species in each park.

0.34‰, respectively. However, at AHL, the lowest $\delta^{15}N$ value was −0.66‰ ± 1.36‰ for Lepidoptera. The highest $\delta^{15}N$ values were recorded for spiders, with values of 5.53‰ ± 0.20‰ (AHL), 5.06‰ ± 0.69‰ (CPL), and 4.14‰ ± 0.04‰ (LCG), respectively (Table 1 and Fig. 2a).

The $\delta^{13}C$ values of green-backed tit nestling feathers from CPL, LCG, and AHL were quite similar, with average values of −25.6‰ ±0.57‰, −25.0‰ ±0.32‰, and −25.0‰ ±0.70‰, respectively (Table 1 and Fig. 2b). For invertebrates, $\delta^{13}C$ value ranges were as follows: 30.9‰ ±0.90‰ (Lepidoptera) to −20.6‰ ±1.67‰ (mantis) at CPL, −30.5‰ ±1.73‰ (lepidoptera) to −21.2‰ ±0.47‰ (mantis) at LCG, and −29.6‰ ±1.26‰ (lepidoptera) to −22.4‰ ±0.58‰ (orthoptera) at AHL. In all three parks, Lepidoptera exhibited the lowest average value among the invertebrates.

3.1.2. *Trophic structure*

Fig. 2c and Table S3 present the differences in the nutrient ecological niches in the food webs of the three parks. CPL exhibited the largest CR value (14‰), followed by LCG (CR = 12‰). The lowest CR value was documented at AHL (9.5‰), suggesting the presence of abundant and diverse food sources in CPL. Conversely, AHL showed the highest NR value (8.2‰), followed by CPL (NR = 6.1‰), with LCG having the lowest NR value (4.2‰), indicating greater distinctions among the three parks. The trophic diversity of AHL (CD = 26.27) was slightly higher than that of CPL (CD = 25.43) and LCG (CD = 25.39). Furthermore, CPL (MNND = 0.23) and AHL (MNND = 0.23) had higher trophic redundancy than LCG (MNND = 0.11). Within the isotopic niche, species distribution was more even in both AHL (SDNND = 0.001) and CPL (SDNND = 0.08) than in LCG (SDNND = 0.11). Moreover, the total degree of trophic diversity was larger for CPL (TA = 43.64) than for AHL (TA = 39.05) and LCG (TA = 33.04). Finally, the SEAc values were comparable and high among the three parks, indicating intensive competition among the biomes in the food webs (Hilgendag et al., 2022; Layman et al., 2007).

Considering the fractionation of stable isotopes of mean values, the differences in carbon and nitrogen isotopes ($\Delta^{13}C$, $\Delta^{15}N$) between feathers and lepidoptera (the lowest trophic level) at the three sites showed that $\Delta^{13}C$ was −5.3‰ (CPL), −5.5‰ (LCG), and −5.0‰ (AHL), while $\Delta^{15}N$ was 3.07‰ (CPL), 2.85‰ (LCG), and 3.01‰ (AHL). These results indicate that there were no significant differences in the

fractionation of stable isotopes among the three locations ($p > 0.05$). When considering extreme values, $\Delta^{13}C$ was −7.1‰ (CPL), −7.3‰ (LCG), and −7.3‰ (AHL), while $\Delta^{15}N$ was 5.04‰ (CPL), 4.21‰ (LCG), and 5.78‰ (AHL). This suggests that while there was no difference in carbon isotope fractionation ($p > 0.05$), there was a significant difference in nitrogen isotope fractionation ($p < 0.05$). This finding indicates that nitrogen isotopes can serve as a valuable metric, at least at the trophic level, for evaluating food web structure based on niche.

3.2. Nestling diet composition and contribution ratios

3.2.1. Diet composition identification via LVO

Among the three forest parks, 117 h of the video records of the parental brood rearing of green-backed tits were achieved. The details are presented in **SI**. In the brood-rearing video records, 951 feedings were recorded, with an average of 8.1 feedings per hour. In total, 856 feedings were effectively identified, and the identification percentages were as follows: 90.3% (n = 624), 89% (n = 137), and 89.6% (n = 95) for CPL, LCG, and AHL, respectively. Ninety-five feedings were not identified, accounting for 9.7%–11.0% of the total nestling diets in these three parks.

The effectively identified food items from the three forest parks included eight invertebrate species: caterpillars, moths, wasp spiders (*Argiope bruennichi*), white-fronted cancer spiders (*Heteropoda venatoria*), small spiders (unknown name), grasshoppers, katydids, and mantis. These eight species were further divided and classified into four major groups based on their characteristics: Lepidoptera (caterpillars and moths), spiders (wasp spiders, white-fronted cancer spiders, and small spiders), Orthoptera (grasshoppers and katydids), and Mantises.

3.2.2. Contribution ratios

LVO. Fig. 3a presents that Lepidoptera was the dominant food composition of green-backed tit nestlings in the three parks, with the following proportions: 74.0% (CPL), 84.4% (LCG), and 63.2% (AHL). These results are consistent with those of great tit nestlings (67.3%) in China (Luo et al., 2020) and great tit nestling diets (75%) in UK (Wilkin et al., 2009). Lepidoptera larvae was also identified as the primary diet of songbirds' nestlings in various countries worldwide, including Spain (García-Navas et al., 2015), Poland (Tomasz and Grzegorz, 2017), Hungary (Sinkovics et al., 2021), and Finland (Eeva et al., 1997, 2003). The dietary proportion of Orthoptera was as follows: 9.3% (CPL), 2.0% (LCG), and 15.0% (AHL). The dietary proportion of spiders was 6.9% (CPL), 2.0% (LCG), and 5.7% (AHL). However, the dietary proportion of mantis was low: 0.1% (CPL), 0.6%(LCG), and 5.7% (AHL).

BIMM. Fig. 3b summarize that Lepidoptera comprised 62.7% ± 4.8% (CPL), 58.9% ± 4.4% (LCG), and 61.4% ± 6.4% (AHL) of the nestling food composition. These results are comparable with those recently reported by Xu et al. (2023b) in a remote forest (67.1% ± 9.1%). Furthermore, the dietary proportions of spiders were similar at CPL (21.0% ± 6.8%) and LCG (23.6% ± 5.6%) but lower at AHL (8.0% ± 4.7%). Moreover, the dietary proportion of mantis was the highest at AHL (22.1% ± 10.6%) but comparable at LCG and CPL (8.8% ± 4.9% and 5.9% ± 3.4%, respectively). In conclusion, the dietary proportions of Orthoptera were similar in the three parks, ranging from 8.5% ± 4.2%–10.4% ± 6.0%.

3.3. Dietary Hg exposure to nestling birds

3.3.1. Total Hg and MeHg concentrations

Nestling feathers. Fig. 4 summarize the THg and MeHg concentrations in the nestling feathers in the three parks. The THg concentrations

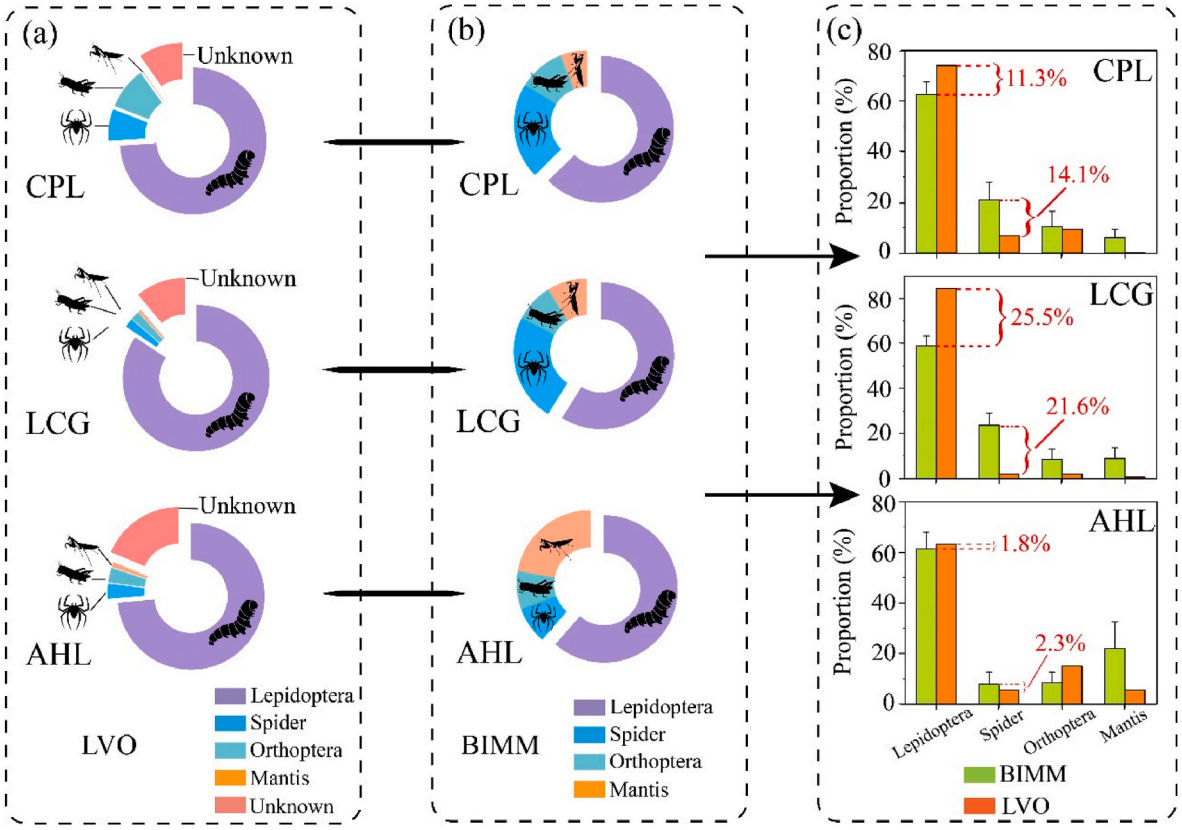

Fig. 3. Dietary compositions of nestlings by LVO and BIMM. (a) The result of LVO (b) the result of BIMM (c) comparison of the two methods, where the left side of each bar chart was the model calculation results and the right side was the video observations. (CPL= Changpoling Forest Park; LCG = Luchongguan Forest Park; AHL = Aha Lake National Wetland Park; LVO= Live videography observation; BIMM= Bayesian isotope mixture model).

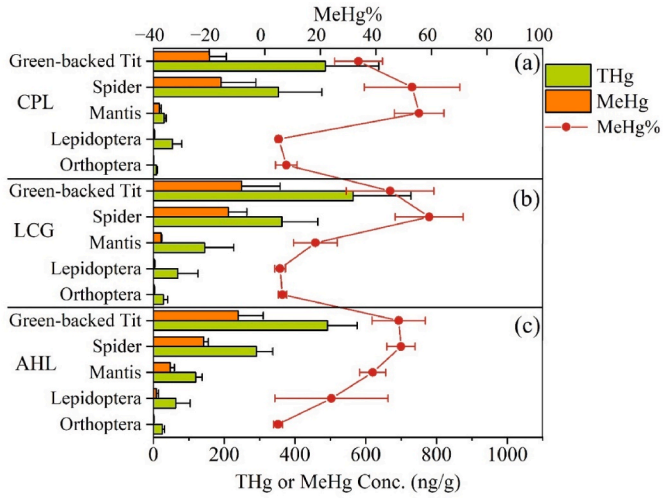

Fig. 4. Concentrations of THg (ng/g), MeHg (ng/g) and MeHg% for all samples. (CPL= Changpoling Forest Park; LCG = Luchongguan Forest Park; AHL = Aha Lake National Wetland Park; THg = Total Hg; MeHg = methylmercury; IHg = inorganic mercury).

in the green-backed tit nestling feathers from LCG, AHL, and CPL were 564 ± 163, 491 ± 84, and 486 ± 151 ng/g, respectively. The average THg concentrations in the nestling feathers in the three parks are comparable with those reported by Zhang et al. (2022) for green-backed tits from CPL (521 ± 156 ng/g) but slightly higher than those in great/-Japanese tit nestling reported by Luo et al. (2020), Su et al. (2021), and Xu et al. (2023b), which were 175.1 ± 191.4, 300 ± 220, and 412 ± 104 ng/g, respectively. Conversely, MeHg concentrations in green-backed tit nestling feathers exhibited slight variations among the three parks, with higher concentrations of 249 ± 109 and 239 ± 71 ng/g observed at LCG and AHL, respectively, in comparison to 158 ± 47 ng/g at CPL. The average MeHg% (34% ± 8.6%–48% ± 9.6%) observed in the nestling feathers in the three parks was slightly higher than MeHg% in the feathers of terrestrial forest birds reported by Luo et al. (2020) (great tit: 26.2% ± 12.0%), Zhang et al. (2022) (green-backed tit: 24% ± 11%), and Xu et al. (2023b) (great tit: 20.0% ± 7.7%).

Invertebrates. Among all the invertebrates in the three parks, spiders had the highest THg and MeHg concentrations (291 ± 46–363 ± 101 and 141 ± 14–211 ± 53 ng/g, respectively). Additionally, the MeHg percentage in spiders (49% ± 5.1%–59% ± 12%) exceeded that in nestling feathers (34% ± 8.6%–48% ± 9.6%) (Fig. 4). The elevated MeHg concentrations observed in spiders may be attributed to their higher trophic positions (indicated by the highest $\delta^{15}N$ value) and their ability to undergo significant MeHg enrichment within the food chains. Nonetheless, the average THg concentrations in Lepidoptera did not exhibit significant differences among the three parks. However, MeHg and MeHg% were higher at AHL compared to the other two parks. This discrepancy may be attributed to the higher trophic diversity (CD) and species distribution (SDNND) at AHL compared to the other two sites, indicating differences in the ecological environment that led to greater MeHg accumulation in biota. The THg and MeHg concentrations in mantis were significantly lower at CPL than at the other two parks; however, MeHg% was the highest at CPL compared with the other two parks. The average THg and MeHg concentrations in Orthoptera were higher at LCG (28 ± 11 and 2.0 ± 1.3 ng/g, respectively) and AHL (25 ± 7.1 and 1.2 ± 0.4 ng/g, respectively) than at CPL (8.4 ± 2.2 and 0.6 ± 0.3 ng/g, respectively). Nevertheless, MeHg% was comparable (4.8% ± 1.6%–7.8% ± 3.9%).

3.3.2. Hg daily intakes of nestlings

Based on the total DIR, diet composition, and Hg concentration in nestlings, the MDIs of THg (MDI_{THg}), MeHg (MDI_{MeHg}), and IHg (MDI_{IHg}) to nestlings and the MDI percentage of each diet composition were estimated; the results are presented in Table S6.

The total MDI_{THg} of the nestling diets was 413.5 ng/day (CPL), 520.1 ng/day (LCG), and 329.6 ng/day (AHL). At CPL, Lepidoptera (126 ng/day) and spiders (277.5 ng/day) contributed the highest to MDI_{THg}, accounting for 97.6% of the total MDI_{THg} of the nestlings. Similar findings were observed at LCG, where Lepidoptera (148.9 ng/day) and spiders (315.3 ng/day) constituted 89.2% of the total MDITHg intake of the nestlings. In contrast, due to the markedly distinct ecological conditions, the nestlings at AHL displayed more intricate diets during their parental brood rearing. Besides Lepidoptera (143.5 ng/day) and spiders (85.1 ng/day), mantis (96.4 ng/day) also became an important dietary item for THg exposure, with the three food items accounting for 97.7% of the total MDI_{THg} of the nestlings.

The estimated MDI_{MeHg} of the nestlings was 160.2, 197.4, and 99.4 ng/day at CPL, LCG, and AHL, respectively. At both CPL and LCG, spiders were the main dietary contributor, accounting for 93.6% and 92.9% of the total MDI_{MeHg} of the nestlings, respectively; in contrast, at AHL, both spiders (41.3 ng/day) and mantis (38.6 ng/day) became the main contributors, accounting for 80.3% of the total MDI_{THg} of the nestlings. For MDI_{IHg}, Lepidoptera and spiders were the main contributors at CPL and LCG, with high contributions of 97.7% and 85%, respectively. Nonetheless, at AHL, mantis also emerged as a significant contributor, contributing to 96.9% of the total MDI_{IHg} intake of the nestlings, alongside Lepidoptera and spiders. These findings indicate that Lepidoptera and spiders serve as the primary sources of dietary IHg exposure, with the latter also playing a vital role in MeHg exposure.

4. Discussion

4.1. Comparison between LVO and BIMM

Both LVO and BIMM revealed that Lepidoptera was the dominant dietary item of green-backed tit nestlings; however, they had different dietary contribution ratios. The contribution ratios of Lepidoptera calculated using BIMM were generally lower than those calculated using LVO, with differences of 11.3% (CPL), 25.5% (LCG), and 1.8% (AHL). Interestingly, when compared to the estimated results by LVO, the BIMM results showed higher concentrations in spiders, and these differences were similar to the reductions observed in Lepidoptera across the three parks: 14.1% (CPL), 21.6% (LCG), and 2.3% (AHL) (Fig. 3c). These findings suggest the important role of spiders in the dietary composition of green-backed tit nestlings.

Robinson et al. (2018) have reported a significant discrepancy in the food compositions of Arctic peregrine falcon nestlings between BIMM (SIAR) and the infrared-sensitive camera video technique. They observed that using video records, the primary diet of Arctic peregrine falcons was insectivorous birds; however, the primary diet was lemmings using the SIAR model. They postulated that the variation in spatial factors and the compositions of δ13C and δ15N in the prey might have contributed to this disparity. Therefore, explaining the different contribution ratios between BIMM and LVO in our data may contribute to the significantly wide range of $\delta^{13}C$ and $\delta^{15}N$ compositions in potentially natural food items.

Moreover, in the present study, another possible reason was that BIMM calculations were based on only the four main food categories identified by LVO, i.e., approximately 9.7%–11.0% of the unidentified items were not included in model processing. Numerous studies have consistently reported that spiders constitute the primary food choice for passerines when feeding their nestlings during the early stages of development (Beaubien et al., 2020; Howie et al., 2018; Samplonius et al., 2016; Serrano-Davies and Sanz, 2017) since spiders could offer the specific nutritional components essential for the growth phase of nestlings (García-Navas et al., 2015; Tomasz and Grzegorz, 2017). Comparing these two methods, the decreased proportions of the diet sources accounted for Lepidoptera were similar to the increased values

for spiders. This suggests that the unidentified food items primarily comprised spiders.

Therefore, we hypothesize that the differences in dietary $\delta^{13}C$ and $\delta^{15}N$ compositions combined with the presence of unidentified items lead to differences between the two methods. Furthermore, we suggest that the former was the primary factor affecting the proportion of dietary contributions. Nevertheless, using LVO to identify dominant food types, then to apply BIMM to calculate the dietary contribution may provide more accurate results.

4.2. Variations in THg and MeHg among the three parks

Significant variations of THg in nestling feathers existed among the three parks, with the mean value at LCG being higher than those at CPL and AHL ($p < 0.001$; $p < 0.05$, Fig. S2). Significantly higher MeHg concentrations ($p < 0.0001$, Fig. S2) were observed in the nestling feathers at LCG and AHL compared to CPL.

Videographic observations and model analyses revealed consistent feeding behaviors of nestlings across the three parks. Therefore, the differences in Hg concentrations in terrestrial birds may be linked to their habitats. The ecological metrics differences provided evidence that the food web structures differed at the three study sites. Notably, there are water bodies near the LCG and AHL sites, and aquatic environments tend to have enriched $\delta^{13}C$ values (less negative $\delta^{13}C$, i.e., more positive $\delta^{13}C$ values) (Post, 2002). The $\delta^{13}C$ values in nestling feathers at LCG and AHL were consistent ($p > 0.05$) and significantly more positive than those at CPL ($p < 0.05$), indicating differences in the underlying carbon sources of their diets.

Although nestlings at all three sites had the same type of diet, nestlings at LCG and CPL likely consumed a greater proportion of prey from aquatic environments. Owing to the nearby water body, which is available for Hg methylation, resulting in increased MeHg levels in the surrounding organisms, particularly riparian spiders, which were then transferred to the nestlings via food chains (Cristol et al., 2008; Tsui et al., 2012). This clarifies why the MeHg concentration in the nestling feathers at LCG and AHL was noticeably higher compared to that at CPL.

4.3. Differences in dietary IHg and MeHg contribution

The high IHg contribution ratios (range: 61.3%–69.8%) suggest that green-backed tit nestlings have heavier body IHg than the MeHg burden via the dietary pathway (Fig. 5). The low average MeHg% (34%–48%) observed in the nestling feathers in this study also revealed heavier body IHg loadings; this is similar to the findings in a remote pine forest (Xu et al., 2023a).

In the present study, Lepidoptera was the main food source for green-backed tit nestlings, with a range of 58.9% ± 4.4%–62.7% ± 4.8%; however, it was not the highest contributor to MeHg exposure owing to the lower contribution of 3.3%–19.3%. In contrast to the proportion of Lepidoptera, the proportion of spiders (8.0% ± 4.7%–23.6% ± 5.6%) in the food sources was lower. However, the contribution of MeHg through the consumption of spiders was the highest, particularly at CPL (93.6%) and LCG (92.9%) (Figs. 3 and 5).

The $\delta^{15}C$ values indicated that Lepidoptera occupied a lower trophic level in the food chain, with limited biomagnification and bioaccumulation of MeHg. In contrast, spiders were situated at the top of the food chain, even higher than birds, exhibiting more complex feeding habits, and substantial biomagnification and bioaccumulation of MeHg. This resulted in a greater MeHg supply to nestlings through their consumption of spiders. This suggests that spiders play a vital role in the MeHg intake of green-backed tit nestlings, even in terrestrial food chains. This finding is consistent with that of previous studies, considering that spiders are a vital source of Hg exposure in birds (Ai et al., 2019; Beaubien et al., 2020; Cristol et al., 2008; Hall et al., 2020). It is worth noting that while spiders offer nestlings the specific nutritional components required for growth, they also elevate the risk of MeHg exposure (García-Navas et al., 2015; Tomasz and Grzegorz, 2017).

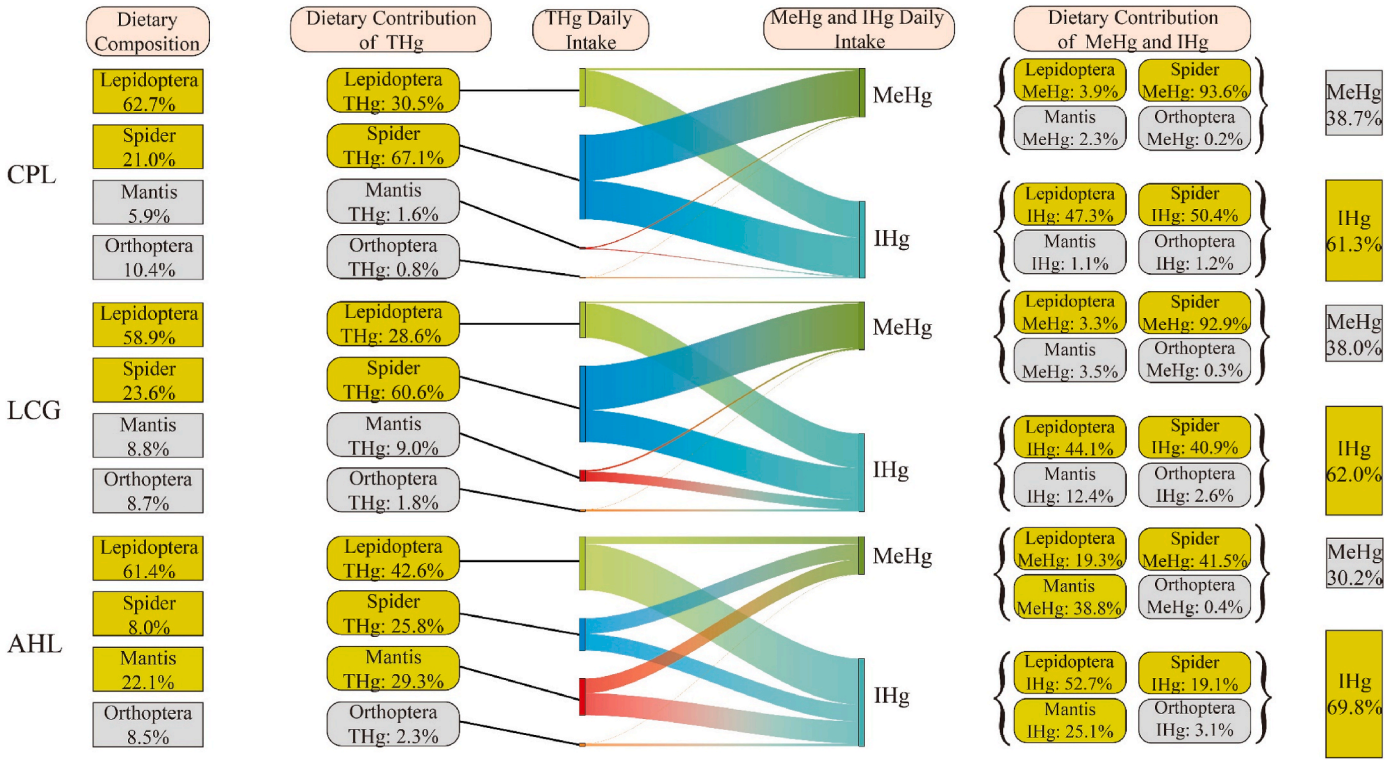

Fig. 5. The proportion of MDIs of THg, MeHg and IHg for dietary composition. The values in the boxes indicated the contribution of dietary composition and MDIs of THg, MeHg and IHg, respectively. The yellow padding indicated the main composition of each part. (CPL= Changpoling Forest Park; LCG = Luchongguan Forest Park; AHL = Aha Lake National Wetland Park; THg = Total Hg; MeHg = methylmercury; IHg = inorganic mercury).

4.4. Environmental implications

Maternal transfer and dietary exposure can contribute to Hg in nestlings (Ackerman et al., 2011). In general, almost all the Hg in eggs is present as MeHg (96.4%) (Ackerman et al., 2013). In the present study, we also observed increased MeHg% (CPL: 82.4% ± 8.8% and LCG: 86.3% ± 3.9%, Table S7) in green-backed tit eggs from these urban forest parks. This result is comparable with that of Xu et al. (2023b), who recently reported a MeHg ratio of as high as 94.2% ± 12.0% in the eggs of great tits living in highly contaminated Hg mines. In summary, the findings presented above imply that the primary route of maternal Hg transfer to green-backed tit nestlings is predominantly through MeHg, and the maternal transfer of MeHg is a significant contributor to the MeHg exposure of nestlings (Abeysinghe et al., 2017; Ackerman et al., 2020).

However, compared with the high MeHg% in eggs, considerably lower MeHg ratios (34%–45%) were observed in nestling feathers in this study. Fig. 5 demonstrates that the IHg form dominates the dietary Hg of nestlings, accounting for 61.3% (CPL), 62.0% (LCG), and 69.8% (AHL) of the content. As both the food intake rate and body weight remained stable when nestlings were approximately 14 days old, the acquired dietary pathway for inorganic IHg is likely the reason for the relatively lower MeHg% in nestling feathers. This observation aligns with the findings of a study on great tit nestlings conducted in another pine forest (Xu et al., 2023a). This phenomenon may indicate that the high MeHg ratios in eggs brought by the mother are bio-diluted by dietary IHg. In future studies, both maternal transfer and dietary pathways should be considered to evaluate the origin of Hg in nestlings. It is important to recognize that the calculation focused solely on dietary route Hg exposure, and the total Hg exposure remains unknown. Given the presence of parental transfer, nestlings are likely exposed to elevated levels of Hg, warranting further investigation in this regard.

The use of isotopic Hg composition to trace Hg origin and biota processes has rapidly grown over the decade. Previous studies have reported the absence of mass-independent fractionation (MIF, Δ^{199}Hg/Δ^{201}Hg) for trophic transfer within the food chain (Kwon et al., 2013, 2014); therefore, the MIF of Hg isotopes may be a reliable tool for tracing biological Hg sources. In addition, this technique has become an effective tracer to study the Hg origin in eggs, internal tissues, blood, and bird feathers (Day et al., 2012; Renedo et al., 2018; Tsui et al., 2018; Xu et al., 2023a, 2023b). Therefore, characterizing the isotopic Hg compositions of food items and eggs can help better understand the biogeochemical processes and contributions that lead to high IHg ratios in green-backed tit nestlings.

5. Conclusions

Our study on dietary compositions and their contribution to green-backed tit nestlings sheds light on Hg origin and Hg accumulation and exposure in songbirds. In three small forest parks, we performed LVO and identified four main types of nestling food items. The estimated daily dietary intakes of Hg using BIMM revealed that Lepidoptera is the main diet of green-backed tit nestlings, whereas Lepidoptera and spiders are the main Hg contributors. Despite spiders not being the primary food source for nestlings, their MeHg contribution through the nestling diets accounted for the majority of the total MeHg burden, presenting a significant risk to nestlings during their growth phase. The proportion of IHg was higher in the nestling diet, and Lepidoptera and spiders were the primary sources of exposure to IHg. Therefore, dietary IHg transfer is important for evaluating the effects of the Hg sources of nestlings. The using of incorporated LVO and BIMM technique to evaluate the diet-specific contribution of IHg and MeHg exposure to nestlings can yield a more desirable result.

Fundings

This work was supported by the National Natural Science Foundation of China (82060850, 42103080); the Science and Technology Program of Guizhou Province: the Hundred Talent Project of Guizhou Province High-Level Innovation Talent Training Plan (QianKeHe Platform Talent [2020]6016-2). We also appreciate the Forestry Administration of Guiyang City, Guizhou Province, Duxi Forestry and Shunhai Forestry for their strong support in the installation and management of nest boxes.

Credit author statement

Chan Li: Investigation, Methodology. Zhidong Xu: Conceptualization, Funding acquisition, Writing – review & editing. Dongya Jia: Investigation, Methodology. Gaoen Wu: Data curation, Investigation. Hongjiang Liu: Data curation, Investigation. Zhuo Chen: Supervision, Writing – review & editing. Guangle Qiu: Conceptualization, Funding acquisition, Supervision, Writing – review & editing. Shenghao Li: Conceptualization, Data curation, Investigation, Methodology, Visualization, Writing – original draft. Fudong Zhang: Data curation, Investigation, Methodology. Longchao Liang: Data curation, Methodology. Jiemin Liu: Conceptualization, Methodology, Writing – review & editing.

Declaration of competing interest

The authors declare that they have no known competing financial interests or personal relationships that could have appeared to influence the work reported in this paper.

Data availability

Data will be made available on request.

Acknowledgements

This work was supported by the National Natural Science Foundation of China (82060850, 42103080); the Science and Technology Program of Guizhou Province: the Hundred Talent Project of Guizhou Province High-Level Innovation Talent Training Plan (QianKeHe Platform Talent [2020]6016-2). We also appreciate the Forestry Administration of Guiyang City, Guizhou Province, Duxi Forestry and Shunhai Forestry for their strong support in the installation and management of nest boxes.

Appendix A. Supplementary data

Supplementary data to this article can be found online at https://doi.org/10.1016/j.envres.2023.117902.

References

Abeysinghe, K.S., Qiu, G., Goodale, E., Anderson, C.W.N., Bishop, K., Evers, D.C., et al., 2017. Mercury flow through an Asian rice-based food web. Environ. Pollut. 229, 219–228. https://doi.org/10.1016/j.envpol.2017.05.067.

Ackerman, J.T., Eagles-Smith, C.A., Herzog, M.P., 2011. Bird mercury concentrations change rapidly as chicks age: toxicological risk is highest at hatching and fledging. Environ. Sci. Technol. 45, 5418–5425. https://doi.org/10.1021/es200647g.

Ackerman, J.T., Herzog, M.P., Schwarzbach, S.E., 2013. Methylmercury is the predominant form of mercury in bird eggs: a synthesis. Environ. Sci. Technol. 47, 2052–2060. https://doi.org/10.1021/es304385y.

Ackerman, J.T., Herzog, M.P., Evers, D.C., Cristol, D.A., Kenow, K.P., Heinz, G.H., et al., 2020. Synthesis of maternal transfer of mercury in birds: implications for altered toxicity risk. Environ. Sci. Technol. 54, 2878–2891. https://doi.org/10.1021/acs.est.9b06119.

Agency, U., 1993. Wildlife Exposure Factors Handbook.

Ai, S., Yang, Y., Ding, J., Yang, W., Bai, X., Bao, X., et al., 2019. Metal exposure risk assessment for tree sparrows at different life stages via diet from a polluted area in northwestern China. Environ. Toxicol. Chem. 38, 2785–2796. https://doi.org/10.1002/etc.4576.

Beaubien, G.B., Olson, C.I., Todd, A.C., Otter, R.R., 2020. The spider exposure pathway and the potential risk to arachnivorous birds. Environ. Toxicol. Chem. 39, 2314–2324. https://doi.org/10.1002/etc.4848.
Cristol, D.A., Brasso, R.L., Condon, A.M., Fovargue, R.E., Friedman, S.L., Hallinger, K.K., et al., 2008. The movement of aquatic mercury through terrestrial food webs. Science 320, 335. https://doi.org/10.1126/science.1154082.
Day, R.D., Roseneau, D.G., Berail, S., Hobson, K.A., Donard, O.F.X., Vander Pol, S.S., et al., 2012. Mercury stable isotopes in seabird eggs reflect a gradient from terrestrial geogenic to oceanic mercury reservoirs. Environ. Sci. Technol. 46, 5327–5335. https://doi.org/10.1021/es2047156.
Driscoll, C.T., Mason, R.P., Chan, H.M., Jacob, D.J., Pirrone, N., 2013. Mercury as a global pollutant: sources, pathways, and effects. Environ. Sci. Technol. 47, 4967–4983. https://doi.org/10.1021/es305071v.
Eeva, T., Lehikoinen, E., Nikinmaa, M., 2003. POLLUTION-INDUCED nutritional stress in birds: an experimental study of direct and indirect effects. Ecol. Appl. 13, 1242–1249. https://doi.org/10.1890/01-5375.
Eeva, T., Lehikoinen, E., Pohjalainen, T., 1997. POLLUTION-RELATED variation in food supply and breeding success in two hole-nesting passerines. Ecology 78, 1120–1131. https://doi.org/10.1890/0012-9658(1997)078[1120:PRVIFS]2.0.CO, 2.
García-Navas, V., Ferrer, E.S., Sanz, J.J., 2015. Prey choice, provisioning behaviour, and effects of early nutrition on nestling phenotype of titmice. Ecoscience 20, 9–18. https://doi.org/10.2980/20-1-3545.
Hall, L.A., Woo, I., Marvin-DiPasquale, M., Tsao, D.C., Krabbenhoft, D.P., Takekawa, J. Y., et al., 2020. Disentangling the effects of habitat biogeochemistry, food web structure, and diet composition on mercury bioaccumulation in a wetland bird. Environ. Pollut. 256, 113280 https://doi.org/10.1016/j.envpol.2019.113280.
Hammerschmidt, C.R., Fitzgerald, W.F., 2005. Methylmercury in mosquitoes related to atmospheric mercury deposition and contamination. Environ. Sci. Technol. 39, 3034–3039. https://doi.org/10.1021/es0485107.
Hartman, C.A., Ackerman, J.T., Herzog, M.P., 2019. Mercury exposure and altered parental nesting behavior in a wild songbird. Environ. Sci. Technol. 53, 5396–5405. https://doi.org/10.1021/acs.est.8b07227.
Hilgendag, I.R., Swanson, H.K., Lewis, C.W., Ehrman, A.D., Power, M., 2022. Mercury biomagnification in benthic, pelagic, and benthopelagic food webs in an Arctic marine ecosystem. Sci. Total Environ. 841, 156424 https://doi.org/10.1016/j.scitotenv.2022.156424.
Hintelmann, H., Nguyen, H.T., 2005. Extraction of methylmercury from tissue and plant samples by acid leaching. Anal. Bioanal. Chem. 381, 360–365. https://doi.org/10.1007/s00216-004-2878-5.
Howie, M.G., Jackson, A.K., Cristol, D.A., 2018. Spatial extent of mercury contamination in birds and their prey on the floodplain of a contaminated river. Sci. Total Environ. 630, 1446–1452. https://doi.org/10.1016/j.scitotenv.2018.02.272.
Hyodo, F., 2015. Use of stable carbon and nitrogen isotopes in insect trophic ecology. Entomol. Sci. 18, 295–312. https://doi.org/10.1111/ens.12128.
Iezekiel, S., Yosef, R., Themistokleus, C., Bakaloudis, D.E., Vlachos, C.G., Antoniou, A., et al., 2021. Endemic Cyprus scops owl Otus cyprius readily breeds in artificial nest boxes. Animals 11. https://doi.org/10.3390/ani.11061775.
Jackson, A.K., Evers, D.C., Etterson, M.A., Condon, A.M., Folsom, S.B., Detweiler, J., et al., 2011a. Mercury exposure affects the reproductive success of a free-living terrestrial songbird, the Carolina Wren (Thryothorus ludovicianus). The Auk 128, 759–769. https://doi.org/10.1525/auk.2011.11106.
Jackson, A.L., Inger, R., Parnell, A.C., Bearhop, S., 2011b. Comparing isotopic niche widths among and within communities: SIBER - stable Isotope Bayesian Ellipses in R. J. Anim. Ecol. 80, 595–602. https://doi.org/10.1111/j.1365-2656.2011.01806.x.
Kwon, S.Y., Blum, J.D., Chen, C.Y., Meattey, D.E., Mason, R.P., 2014. Mercury isotope study of sources and exposure pathways of methylmercury in estuarine food webs in the Northeastern U.S. Environ. Sci. Technol. 48, 10089–10097. https://doi.org/10.1021/es5020554.
Kwon, S.Y., Blum, J.D., Chirby, M.A., Chesney, E.J., 2013. Application of mercury isotopes for tracing trophic transfer and internal distribution of mercury in marine fish feeding experiments. Environ. Toxicol. Chem. 32, 2322–2330. https://doi.org/10.1002/etc.2313.
Lavoie, R.A., Jardine, T.D., Chumchal, M.M., Kidd, K.A., Campbell, L.M., 2013. Biomagnification of mercury in aquatic food webs: a worldwide meta-analysis. Environ. Sci. Technol. 47, 13385–13394. https://doi.org/10.1021/es403103t.
Layman, C.A., Arrington, D.A., Montaña, C.G., Post, D.M., 2007. Can stable isotope ratios provide for community-wide measures of trophic structure? Ecology 88, 42–48. https://doi.org/10.1890/0012-9658 (2007)88[42:Csirpf]2.0.Co;2.
Li, C., Xu, Z., Luo, K., Chen, Z., Xu, X., Xu, C., et al., 2021. Biomagnification and trophic transfer of total mercury and methylmercury in a sub-tropical montane forest food web, southwest China. Chemosphere 277, 130371. https://doi.org/10.1016/j.chemosphere.2021.130371.
Lindqvist, O., Johansson, K., Bringmark, L., Timm, B., Aastrup, M., Andersson, A., et al., 1991. Mercury in the Swedish environment ? Recent research on causes, consequences and corrective methods. Water, Air, Soil Pollut. 55, xi–261. https://doi.org/10.1007/bf00542429.
Luo, K., Xu, Z.D., Wang, X., Quan, R.C., Lu, Z.Y., Bi, W.Q., et al., 2020. Terrestrial methylmercury bioaccumulation in a pine forest food chain revealed by live nest videography observations and nitrogen isotopes. Environ. Pollut. 263, 114530 https://doi.org/10.1016/j.envpol.2020.114530.
Pagani-Núñez, E., Renom, M., Mateos-Gonzalez, F., Cotín, J., Senar, J.C., 2017. The diet of great tit nestlings: comparing observation records and stable isotope analyses. Basic Appl. Ecol. 18, 57–66. https://doi.org/10.1016/j.baae.2016.11.004.
Pagani-Núñez, E., Senar, J.C., 2013. One hour of sampling is enough: great tit Parus major parents feed their nestlings consistently across time. Acta Ornithol. (Warszaw) 48, 194–200. https://doi.org/10.3161/000164513X678847, 7.
Parnell, A.C., Inger, R., Bearhop, S., Jackson, A.L., 2010. Source partitioning using stable isotopes: coping with too much variation. PLoS One 5, e9672. https://doi.org/10.1371/journal.pone.0009672.
Parnell, A.C., Phillips, D.L., Bearhop, S., Semmens, B.X., Ward, E.J., Moore, J.W., et al., 2013. Bayesian stable isotope mixing models. Environmetrics 24.
Ponton, D.E., Lavoie, R.A., Leclerc, M., Bilodeau, F., Planas, D., Amyot, M., 2021. Understanding food web mercury accumulation through trophic transfer and carbon processing along a river affected by recent run-of-river dams. Environ. Sci. Technol. 55, 2949–2959. https://doi.org/10.1021/acs.est.0c07015.
Post, D.M., 2002. Using stable isotopes to estimate trophic position: models, methods, and assumptions. Ecology 83, 703–718. https://doi.org/10.1890/0012-9658(2002)083[0703:Usitet]2.0.Co, 2.
Renedo, M., Amouroux, D., Duval, B., Carravieri, A., Tessier, E., Barre, J., et al., 2018. Seabird tissues as efficient biomonitoring tools for Hg isotopic investigations: implications of using blood and feathers from chicks and adults. Environ. Sci. Technol. 52, 4227–4234. https://doi.org/10.1021/acs.est.8b00422.
Renedo, M., Bustamante, P., Tessier, E., Pedrero, Z., Cherel, Y., Amouroux, D., 2017. Assessment of mercury speciation in feathers using species-specific isotope dilution analysis. Talanta 174, 100–110. https://doi.org/10.1016/j.talanta.2017.05.081.
Robinson, B.G., Franke, A., Derocher, A.E., 2018. Stable isotope mixing models fail to estimate the diet of an avian predator. Auk 135, 60–70. https://doi.org/10.1642/Auk-17-143.1.
Samplonius, J.M., Kappers, E.F., Brands, S., Both, C., 2016. Phenological mismatch and ontogenetic diet shifts interactively affect offspring condition in a passerine. J. Anim. Ecol. 85, 1255–1264. https://doi.org/10.1111/1365-2656.12554.
Serrano-Davies, E., Sanz, J.J., 2017. Habitat structure modulates nestling diet composition and fitness of Blue Tits Cyanistes caeruleus in the Mediterranean region. Hous. Theor. Soc. 64, 295–305. https://doi.org/10.1080/00063657.2017.1357678.
Sinkovics, C., Seress, G., Pipoly, I., Vincze, E., Liker, A., 2021. Great tits feed their nestlings with more but smaller prey items and fewer caterpillars in cities than in forests. Sci. Rep. 11, 24161 https://doi.org/10.1038/s41598-021-03504-4.
Su, T., He, C., Jiang, A., Xu, Z., Goodale, E., Qiu, G., 2021. Passerine bird reproduction does not decline in a highly-contaminated mercury mining district of China. Environ. Pollut. 286, 117440 https://doi.org/10.1016/j.envpol.2021.117440.
Surmacki, A., Podkowa, P., 2022. The use of trail cameras to monitor species inhabiting artificial nest boxes. Ecol. Evol. 12, e8550 https://doi.org/10.1002/ece3.8550.
Tomasz, W., Grzegorz, N., 2017. Diet of marsh tit poecile palustris nestlings in a primeval forest in relation to food supply and age of young. Acta Ornithol. (Warszaw) 52, 105–118. https://doi.org/10.3161/00016454AO2017.52.1.010.
Tsui, M.T., Adams, E.M., Jackson, A.K., Evers, D.C., Blum, J.D., Balogh, S.J., 2018. Understanding sources of methylmercury in songbirds with stable mercury isotopes: challenges and future directions. Environ. Toxicol. Chem. 37, 166–174. https://doi.org/10.1002/etc.3941.
Tsui, M.T., Blum, J.D., Finlay, J.C., Balogh, S.J., Nollet, Y.H., Palen, W.J., et al., 2014. Variation in terrestrial and aquatic sources of methylmercury in stream predators as revealed by stable mercury isotopes. Environ. Sci. Technol. 48, 10128–10135. https://doi.org/10.1021/es500517s.
Tsui, M.T., Blum, J.D., Kwon, S.Y., Finlay, J.C., Balogh, S.J., Nollet, Y.H., 2012. Sources and transfers of methylmercury in adjacent river and forest food webs. Environ. Sci. Technol. 46, 10957–10964. https://doi.org/10.1021/es3019836.
Tsui, M.T, Liu, S., Brasso, R.L., Blum, J.D., Kwon, S.Y., Ulus, Y., et al., 2019. Controls of methylmercury bioaccumulation in forest floor food webs. Environ. Sci. Technol. 53, 2434–2440. https://doi.org/10.1021/acs.est.8b06053.
US EPA, 1998. Method 1630: Methylmercury in Water by Distillation, Aqueous Ethylation, Purge and Trap, and CVAFS. U.S. EPA, Washington, D.C, USA, pp. 1–55.
US EPA, 2002. Method 1631: Mercury in Water by Oxidation, Purge and Trap, and Cold Vapor Atomic Fluorescence Spectrometry. U.S. EPA, Washington, D.C, USA, pp. 1–33.
White, A.F., Dawson, R.D., 2021. Can diet composition estimates using stable isotope analysis of feathers predict growth and condition in nestling mountain bluebirds (Sialia currucoides). Ecol. Evol. 11, 15273–15288. https://doi.org/10.1002/ece3.8210.
Wilkin, T.A., King, L.E., Sheldon, B.C., 2009. Habitat quality, nestling diet, and provisioning behaviour in great tits Parus major. J. Avian Biol. 40, 135–145. https://doi.org/10.1111/j.1600-048X.2009.04362.x.
World Health Organization, 2020. 10 Chemicals of Public Health Concern. https://www.who.int/news-room/photo-story/photo-story-detail/10-chemicals-of-public-health-concern.
Wu, X., Zheng, X., Yu, L., Lu, R., Zhang, Q., Luo, X.J., et al., 2022. Biomagnification of persistent organic pollutants from terrestrial and aquatic invertebrates to songbirds: associations with physiochemical and ecological indicators. Environ. Sci. Technol. 56, 12200–12209. https://doi.org/10.1021/acs.est.2c02177.
Xu, Z., Luo, K., Lu, Q., Shang, L., Tian, J., Lu, Z., et al., 2023a. The mercury flow through a terrestrial songbird food chain in subtropical pine forest: elucidated by Bayesian isotope mixing model and stable mercury isotopes. J. Hazard Mater. 459, 132263 https://doi.org/10.1016/j.jhazmat.2023.132263.
Xu, Z., Lu, Q., Xu, X., Liang, L., Abeysinghe, K.S., Chen, Z., et al., 2023b. Aquatic methylmercury is a significant subsidy for terrestrial songbirds: evidence from the odd mass-independent fractionation of mercury isotopes. Sci. Total Environ. 880, 163217 https://doi.org/10.1016/j.scitotenv.2023.163217.
Zabala, J., Rodriguez-Jorquera, I.A., Orzechowski, S.C., Frederick, P., 2019. Mercury concentration in nestling feathers better predicts individual reproductive success than egg or nestling blood in a piscivorous bird. Environ. Sci. Technol. 53, 1150–1156. https://doi.org/10.1021/acs.est.8b05424.
Zhang, F., Xu, Z., Xu, X., Liang, L., Chen, Z., Dong, X., et al., 2022. Terrestrial mercury and methylmercury bioaccumulation and trophic transfer in subtropical urban forest

food webs. Chemosphere 299, 134424. https://doi.org/10.1016/j.chemosphere.2022.134424.